Detection of Two Histidyl Ligands to Cu_A of Cytochrome Oxidase by 35-GHz ENDOR: $^{14,15}N$ and $^{63,65}Cu$ ENDOR Studies of the Cu_A Site in Bovine Heart Cytochrome aa_3 and Cytochromes caa_3 and ba_3 from *Thermus thermophilus*

Ryszard J. Gurbiel,[†,§] Yang-Cheng Fann,[†] Kristene K. Surerus,[‡] Melanie M. Werst,[†] Siegfried M. Musser,[⊥] Peter E. Doan,[†] Sunney I. Chan,[⊥] James A. Fee,[‡,∥] and Brian M. Hoffman*[,†]

Contribution from the Department of Chemistry, Northwestern University, Evanston, Illinois 60208-3113, Los Alamos National Laboratory, Los Alamos, New Mexico 87545, Institute of Molecular Biology, Jagiellonian University, 31-120 Kraków, Poland, Arthur Amos Noyes Laboratory of Chemical Physics, California Institute of Technology, Pasadena, California 91125, and Department of Biology, University of California, La Jolla, California 92093

Received June 1, 1993[⊗]

Abstract: To study the ligation of the Cu_A site of heme–copper terminal oxidases, we have performed ENDOR measurements at X-band (9-GHz) and 35-GHz microwave frequencies on the three titled enzymes. The 35-GHz measurements provide complete spectral separation of the ^1H and ^{14}N resonances and permit analysis of the field dependence of the ^{14}N ENDOR for each enzyme. The results indicate that two nitrogenous ligands were quite unequal hyperfine couplings are ligated to Cu_A in each of the enzymes studied. We have also examined cytochrome caa_3 isolated from His$^-$ *Thermus* cells grown in the presence of D,L-[δ,ϵ-$^{15}N_2$]histidine. The 35-GHz Cu_A ENDOR spectrum of this protein includes ^{15}N ENDOR resonances whose frequencies confirm the presence of two nitrogenous ligands; comparison with the ^{14}N ENDOR spectra further shows that the ligand with the larger hyperfine coupling (N1) displays well-resolved ^{14}N quadrupole splitting. The theory for simulating frozen-solution ENDOR spectra as refined here permits a determination of both hyperfine and quadrupole tensors for N1 of all three enzymes. These indicate that the bonding parameters and geometry of Cu_A are well conserved. These measurements demonstrate unequivocally that two histidylimidazole N atoms are coordinated to Cu_A in the oxidized form of the enzyme and provide a first indication of the site geometry. On the basis of the previously established sequence homology among these heme–copper oxidases, it is likely that the two histidine residues conserved in all subunit II and subunit IIc sequences form part of the Cu_A binding site. The Cu_A sites in the three enzymes are further compared through $^{63,65}Cu$ ENDOR.

Introduction

Terminal oxidases containing heme and copper are widely distributed in nature.[1,2] A subclass of these enzymes, typified by eukaryotic cytochrome aa_3, utilizes two copper centers and two hemes A to translocate protons while oxidizing cytochromes *c* and reducing dioxygen to water.[3] Of the two Cu sites, the Cu_B is EPR silent because of its close proximity to a $heme_A$, is coordinated to at least three histidine residues, participates directly in dioxygen reduction, and appears to possess spectroscopic properties typical of ionic Cu^{2+}. By comparison, the Cu_A site is EPR detectable, possesses very unusual spectroscopic properties, and consequently has been the subject of intense investigation.[4] The oxidized form of this center is characterized by a weak ($\Delta\epsilon_{ox\text{-}red} \simeq 1000$–$2000\ M^{-1}\ cm^{-1}$) optical absorption band centered near 800 nm and by an EPR signal that has surprisingly small *g* shifts ($g_{1,2,3}$ = 2.18, 2.04, 1.99),[5,6] has no apparent Cu hyperfine structure, and depending on other particular preparation of enzymes, has an intensity that corresponds to roughly half the Cu in the sample. These spectral characteristics are the defining features of oxidized Cu_A. Peisach and Blumberg[7] set the tone for research into the properties of Cu_A by noting that the apparent *g*-values are "closer to 2 than any other natural or artificial Cu protein" and suggesting that the "the lack of hyperfine structure may arise from a specific stereochemical distortion of... electron-accepting ligands of the copper or from a significant transfer of the unpaired spin of the copper to sulfur." More recently, Kroneck, Antholine, Zumft, and their co-workers[8,9] have suggested that the Cu_A center actually contains two Cu ions, one formally Cu(I) and the other Cu(II) with electron spin density distributed equally on both metals.[10]

Previous magnetic resonance studies have provided further insight on the atomic composition of the Cu_A site. The observation

† Northwestern University.
‡ Los Alamos National Laboratory.
§ Jagiellonian University.
⊥ California Institute of Technology.
∥ University of California.

⊗ Abstract published in *Advance ACS Abstracts,* October 1, 1993.

(1) *Cf.* Poole, R. K. *Biochim. Biophys. Acta* **1983**, *726*, 205–243.
(2) For review, see: Ludwig, B. *FEMS Microbiol. Rev.* **1987**, *46*, 41–56.
(3) Wikström, M.; Krab, K.; Saraste, M. *Cytochrome Oxidase: A Synthesis*; Academic Press: New York, 1981.
(4) Li, P. M.; Gelles, J.; Chan, S. I. *J. Biol. Chem.* **1987**, *263*, 8420–8429.
(5) Aasa, R.; Albracht, S. P. J.; Falk, K. E.; Lann, B.; Vänngård, T. *Biochim. Biophys. Acta* **1976**, *422*, 260–272.
(6) Froncisz, W.; Scholes, C. P.; Hyde, J. S.; Wei, Yau-H.; King, T. E.; Shaw, R. W.; Beinert, H. *J. Biol. Chem.* **1979**, *254*(16), 7482–7484.
(7) Peisach, J.; Blumberg, W. E. *Arch. Biochem. Biophys.* **1974**, *165*, 691–708.
(8) (a) Kroneck, P. M.; Antholine, W. A.; Riester, J.; Zumft, W. G. *FEBS Lett.* **1989**, *248*(1–2), 212–213. (b) Kroneck, P. M. H.; Antholine, W. E.; Kastrau, D. H. W.; Buse, G.; Steffens, G. C. M.; Zumft, W. G. *FEBS Lett.* **1990**, *268*, 274–276. (c) Antholine, W. E.; Kastrau, D. H.; Steffens, G. C.; Buse, G.; Zumft, W. G.; Kroneck, P. M. *Eur. J. Biochem.* **1992**, *209*(3), 875–881. (d) Kroneck, P. M. H.; Antholine, W. E.; Koteich, H.; Kastrau, D. H. W.; Neese, F.; Zumft, W. G. In *Bioinorganic Chemistry of Copper*; Karlin, K. D., Tyeklár, Z., Eds.; Chapman & Hall: New York, 1993. (e) Malmström, B. G.; Aasa, R. *FEBS Lett.* **1993**, *325*, 49–52.
(9) Li, P. M.; Malmström, B. G.; Chan, S. I. *FEBS Lett.* **1989**, *248*(1–2), 210–211.
(10) For review, see: Fee, J. A.; Antholine, W. E.; Fan, C.; Gurbiel, R. J.; Surerus, K.; Werst, M.; Hoffman, B. M. In *Bioinorganic Chemistry of Copper*; Karlin, K. D., Tyeklár, Z., Eds.; Chapman & Hall: New York, 1993.

0002-7863/93/1515-10888$04.00/0

of $^{63,65}Cu$ ENDOR signals by Hoffman *et al.*[11] unambiguously showed that the Cu_A site contains a Cu that bears appreciable spin density. Scholes and his colleagues recorded X-band ENDOR spectra at two frequencies that revealed at least two different ^1H atoms with fairly large and isotropic couplings of ~12 and 19 MHz while signals in the range of 7–10 MHz were assigned to ^{14}N atoms.[12] Chan, Scholes, and their co-workers attempted to resolve the X-band ENDOR signals by isotope substitution studies ([^{15}N]histidine and [^2H]cysteine) using yeast cytochrome aa_3; they concluded that Cu_A was coordinated to at least one histidine and one cysteine.[13,14] These efforts were severely hindered by the overlap between $^{14,15}N$ and ^1H resonances in ENDOR spectra taken at X-band (~9 GHz).

Here, we examine the ENDOR properties of the Cu_A site in each of three members of the heme–copper oxidase family. Cytochrome *c* oxidase from bovine heart tissue is a multisubunit protein that resides in the inner mitochondrial membrane and is the holotypical form of the enzyme.[3] Cytochrome caa_3 is a two-subunit enzyme isolated from the plasma membrane of the aerobic bacterium *Thermus thermophilus*.[15-21] The smaller of the two subunits is a fusion protein consisting of a typical subunit II fused to that of a typical cytochrome *c* and subunit named IIc.[22] The larger of the two subunits appears to be a fusion protein consisting of a typical subunit I fused to a typical subunit III.[23] Cytochrome ba_3 was initially described as a single subunit enzyme from the same source[24] although recent molecular genetic studies show that ba_3 is also a multisubunit enzyme containing one subunit with a characteristic Cu_A binding site.[25,26] ENDOR measurements at 35 GHz permit the complete separation of ^1H and $^{14,15}N$ resonances, thereby for the first time opening the possibility of a full characterization of the nitrogenous ligands to Cu_A. To explore the coordination environment of Cu_A, we compare and analyze 35-GHz ^{14}N ENDOR signals arising from Cu_A in the three different proteins through the use of the theory of polycrystalline ENDOR spectra[27-29] as refined here and as guided by ^{15}N ENDOR spectra from a sample of cytochrome caa_3 enriched with ^{15}N-labeled histidine. As part of this study, we have also directly examined the hyperfine coupling to Cu in the Cu_A center through X-band $^{63,65}Cu$ ENDOR of the three enzymes.

Procedure and Theory

Proteins. Bovine cytochrome *aa*3 was prepared by the method of Hartzell and Beinert.[30] Cytochromes caa_3 and ba_3 were prepared from *T. thermophilus* cells by the methods of Yoshida *et al.*[20] and Zimmermann,[31] respectively. A mutant strain of *T. thermophilus* HB8 requiring histidine for growth was isolated by Ms. K. Findling in 1982 and will be described elsewhere. Cells were grown in the presence of 1 mM D,L-[δ,ϵ-$^{15}N_2$]histidine in the synthetic medium of Mather and Fee,[32] and cytochrome caa_3 was isolated according to the method of Yoshida *et al.*[20] Labeled histidine was obtained from the Stable Isotope Resource at Los Alamos.

ENDOR Measurements. ENDOR spectra were recorded on a Varian Associates E-109 spectrometer as described previously using either an E109 microwave bridge for X-band (9 GHz) or an E-110 microwave bridge for 35 GHz.[33] For a single orientation of a paramagnetic center, the ENDOR spectrum of a nucleus (J) of spin I consists in principle of $2I$ transitions at frequencies given to the first approximation by eq 1.[34]

$$\nu_{\pm}(m_I) = \left|\pm\frac{A(J)}{2} + \nu(J) + \frac{3P}{2}(J)(2m_I - 1)\right| \quad -I + 1 \le m_I \le I \quad (1)$$

Here, $A(J)$ and $P(J)$ are the angle-dependent hyperfine and quadrupole coupling constants, respectively, which are molecular parameters and independent of the spectrometer microwave frequency, and $\nu(J)$ is the nuclear Larmor frequency $h\nu(J) = g_J\beta_J\mathbf{B}$.[35] For a set of equivalent ^{14}N nuclei [$(I = 1)$, $A(^{14}N)/2 > \nu(^{14}N) > 3P(^{14}N)/2$], eq 1 in principle describes a four-line pattern consisting of a Larmor-split doublet centered at $A(^{14}N)/2$ split by $2\nu(^{14}N)$ and further split by the quadrupole term. The nuclei of ^{15}N have $I = {}^1/_2$, and the ENDOR pattern consists of only a Larmor-split doublet centered at $A(^{15}N)/2$ and split by $2\nu(^{15}N)$. The hyperfine couplings and Larmor frequencies of two nitrogen isotopes obey the relation:

$$\left|\frac{\nu(^{15}N)}{\nu(^{14}N)}\right| = \left|\frac{A(^{15}N)}{A(^{14}N)}\right| = 1.403 \quad (2)$$

Thus, the assignment of an ENDOR spectrum for one isotope directly predicts features of the other one. For ^{63}Cu and ^{65}Cu nuclei ($I = {}^3/_2$), eq 1 predicts a triplet of doublets centered at $A(Cu)/2$ for $A(Cu)/2 > 3P(Cu)/2 > \nu(Cu)$. Because the $^{14,15}N$ and $^{63,65}Cu$ resonances are centered at a molecular parameter, $A/2$, the center of these patterns does not change with the spectrometer frequency.

A set of magnetically equivalent protons ($I = {}^1/_2$) gives a hyperfine-split doublet of ENDOR transitions ($\nu_{\pm}$) that are centered at proton Larmor frequency and split by $A(H)$

$$\nu_{\pm} = \left|\nu(H) \pm \frac{A(H)}{2}\right| \quad (3)$$

where $\nu(H) = g_H\beta_n[\nu(M)/g_{obs}\beta_e]$ varies with the microwave frequency $\nu(M)$. An increase of $\nu(M)$ from 9 GHz (X-band) to 35 GHz increases $\nu(H)$ (at $g \simeq 2$) from 14 to ~53 MHz, which eliminates spectral overlap of the proton signals with the ^{14}N signals. Conversely, copper ENDOR is better performed at X-band frequency to avoid overlap with the ^1H signal at 35 GHz.

Simulation of Polycrystalline ENDOR Spectra. The samples employed in this study were frozen solutions and thus contained a random distribution of all protein orientations. As reviewed in detail,[36-38] the principal values of a nuclear hyperfine tensor and its orientation relative to the **g**-tensor axis frame can be determined by simulating a set of ENDOR spectra recorded at *g*-values (fields) across the EPR envelope. This section

(11) Hoffman, B. M.; Roberts, J. E.; Swanson, M.; Speck, S. H.; Margoliash, E. *Proc. Natl. Acad. Sci. U.S.A.* **1980**, *77*(3), 1452–1456.
(12) Van Camp, H. L.; Wei, Y.-H.; Scholes, C. P.; King, T. E. *Biochim. Biophys. Acta* **1978**, *537*, 238–246.
(13) Stevens, T. H.; Martin, C. T.; Wang, H.; Brudvig, G. W.; Scholes, C. P.; Chan, S. I. *J. Biol. Chem.* **1982**, *257*(20), 12106–12113.
(14) Martin, C. T.; Scholes, C. P.; Chan, S. I. *J. Biol. Chem.* **1988**, *263*(17), 8420–8429.
(15) Fee, J. A.; Findling, K. L.; Lees, A.; Yoshida, T. In *Frontiers in Biological Energetics*; Dutton, P. L., Leigh, J. S., Scarpa, A., Eds.; Academic Press: New York, 1978; Vol. 1, pp 118–126.
(16) Fee, J. A.; Choc, M. G.; Findling, K. L.; Lorence, R.; Yoshida, T. *Proc. Natl. Acad. Sci. U.S.A.* **1980**, *77*, 147–151.
(17) Fee, J. A.; Kuila, D.; Mather, M. W.; Yoshida, T. *Biochim. Biophys. Acta* **1986**, *853*, 153–185.
(18) Ogura, T.; Hon-nami, K.; Oshima, T.; Yoshikawa, S.; Kitagawa, T. *J. Am. Chem. Soc.* **1983**, *105*, 7781–7783.
(19) Hon-nami, K.; Oshima, T. *Biochemistry* **1984**, *23*, 454–460.
(20) Yoshida, T.; Lorence, R. M.; Choc, M. G.; Tarr, G. E.; Findling, K. L.; Fee, J. A. *J. Biol. Chem.* **1984**, *259*, 112–123.
(21) Rusnak, F. M.; Münck, E.; Nitsche, C. I.; Zimmermann, B. H.; Fee, J. A. *J. Biol. Chem.* **1987**, *262*(34), 16328–16332.
(22) Mather, M. W.; Springer, P.; Fee, J. A. *J. Biol. Chem.* **1991**, *266*(8), 5025–5035.
(23) Mather, M. W.; Springer, P.; Hansel, S.; Buse, G.; Fee, J. A. *J. Biol. Chem.* **1993**, *268*, 5395–5408.
(24) Zimmermann, B. H.; Nitsche, C. I.; Fee, J. A.; Rusnak, F.; Münck, E. *Proc. Natl. Acad. Sci. U.S.A.* **1988**, *85*(16), 5779–5783.
(25) Keightley, J. A. Ph.D. Dissertation, University of New Mexico, 1993.
(26) Keightley, J. A. *et al.*, in preparation.
(27) Hoffman, B. M.; Martinsen, J.; Venters, R. A. *J. Magn. Reson.* **1984**, *59*, 110–123.
(28) Hoffman, B. M.; Venters, R. A.; Martinsen, J. *J. Magn. Reson.* **1985**, *62*, 537–542.
(29) Hoffman, B. M.; Gurbiel, R. J.; Werst, M. M.; Sivaraja, M. In *Advanced EPR. Applications in Biology and Biochemistry*; Hoff, A. J., Ed.; Elsevier: Amsterdam, 1989; Chapter 15, pp 541–591.
(30) Hartzell, C. R.; Beinert, H. *Biochim. Biophys. Acta* **1974**, *368*, 318–338.
(31) Zimmermann, B. H. Ph.D. *Dissertation*, University of Michigan (Ann Arbor), 1988.
(32) Mather, M. W.; Fee, J. A. *Plasmid* **1990**, *24*(1), 45–56.
(33) Werst, M. M.; Davoust, C. E.; Hoffman, B. M. *J. Am. Chem. Soc.* **1991**, *113*(5), 1533–1538.
(34) Abragam, A.; Bleaney, B. *Electron Paramagnetic Resonance of Transition Ions*, 2nd ed.; Clarendon Press: Oxford, 1970.
(35) Atherton, N. M. *Electron Spin Resonance. Theory and Applications*; Halsted Press: New York, London, Sydney, Toronto, 1973; Ellis Horwood Series in Physical Chemistry.
(36) Gurbiel, R. J.; Batie, C. J.; Sivaraja, M.; True, A. E.; Fee, J. A.; Hoffman, B. M.; Ballou, D. P. *Biochemistry* **1989**, *28*(11), 4861–4871.
(37) Hoffman, B. M. *Accts. Chem. Res.* **1991**, *24*(6), 164–170.
(38) Hoffman, B. M.; DeRose, V. J.; Doan, P. E.; Gurbiel, R. J.; Houseman, A. L. P.; Telser, J. In *Biological Magnetic Resonance*; Berliner, L., Ed.; Plenum Press: New York, in press.

describes a modification of the general theory of orientation-selective ENDOR for systems with **g**, **A**, and **P** tensors of arbitrary symmetry and relative orientation.[27,28]

Consider the common situation of a frozen solution of a protein with a metal center whose EPR spectrum is described by **g**'-tensor that has rhombic (or axial) symmetry, with $g_1 > g_2 > g_3$, and is without resolved hyperfine structure. ENDOR spectra are taken with the external field fixed within the polycrystalline EPR envelope at a selected value, **B**, which corresponds to a g-value determined by the spectrometer frequency, $g = h\nu/\beta\mathbf{B}$. As recognized by Hyde and his co-workers,[39] ENDOR spectra taken with the magnetic field set at the extreme edges of the frozen-solution EPR envelope, near the maximal or minimal g-values, give single-crystal-like patterns from the subset of molecules for which the magnetic field happens to be directed along a **g**-tensor axis. An ENDOR spectrum obtained using an intermediate field and g-value does not arise from a single orientation of the magnetic field relative to the molecular **g**-tensor coordinate frame; nonetheless, it is associated with a *well-defined* subset of molecular orientations. Ignoring for the moment the existence of a nonzero component EPR line width (employ the EPR envelope of a δ-function component line), the EPR signal intensity, and thus the ENDOR spectrum detected at field **B**, corresponding to $g = h\nu/\beta\mathbf{B}$, is a superposition of the signals from those selected molecular orientations associated with the curve on the unit sphere s_g for which the orientation-dependent spectroscopic splitting factor satisfies the condition $g'(\theta,\phi) = g$. (For illustrations, see ref 37.) However, although g is constant along the curve s_g, the orientation-dependent ENDOR frequencies $\nu_\pm(m)$ (given in first order by eqs 1 and 3) are not. Thus, the ENDOR intensity in a spectrum taken at g is a superposition from the subset of orientations associated with s_g and occurs in a range of frequencies spanning the values of $\nu_\pm$ associated with the subset. The calculation of this resultant intensity superposition is facilitated by a proper choice of independent variables. It is standard practice to choose as independent variables the polar coordinates (θ,ϕ) that describe the orientation of the external field within the **g**-tensor frame. However, as the ENDOR measurement leads us to focus on a curve of constant g, it is advantageous to change independent variables from (θ,ϕ) to (ϕ,g); one can solve eq 3 to give θ as a function of (ϕ,g):

$$\sin^2\theta(\phi,g) = \frac{g^2 - g_3^2}{(g_2^2 - g_3^2) + (g_1^2 - g_2^2)\cos^2\phi} \qquad (4)$$

At any observing g-value within the EPR envelope of a polycrystalline (frozen-solution) sample, the intensity of a superposition ENDOR spectrum at radiofrequency ν can be written as a sum (integral) of contributions from all molecules in the solution for which **B** is oriented such that (θ,ϕ) lies on the curve s_g. In our original formulation, the intensity was taken as a line integral along s_g. We have now determined that it is more appropriate to calculate the superposition ENDOR spectrum associated with a particular g-value along the EPR envelope by an integration of the area element $d\sigma$ associated with the point (ϕ,g) along the curve s_g. We find that

$$d\sigma = \left|\left(\frac{g}{g^2 - g_3^2}\right)\frac{\sin^2\theta(\phi,g)}{\cos\theta(\phi,g)}\right| d\phi\, dg \equiv w(\phi,g)\, d\phi\, dg \qquad (5)$$

where $\sin^2\theta(\phi,g)$ again is given by eq 4. The integral along the curve of constant g then becomes

$${}^{\delta}I(\nu,g) = \sum_m \sum_{\pm} \int_{s_g} L[\nu - \nu_\pm(m)]e(\nu_\pm(m))w(\phi,g)\, d\phi) \qquad (6)$$

where $L(x)$ is an ENDOR line shape function and $e(\nu)$ is the hyperfine enhancement factor.[34,35] For $I = {}^1/_2$, the nuclear transition observed is $m = {}^1/_2 \leftrightarrow m = -{}^1/_2$ and the summation involves only the electron spin quantum number $m_s' = \pm{}^1/_2$; for $I > {}^1/_2$, quadrupole terms must be included and the sum extended over the additional nuclear transitions. In the case of an EPR spectrum that shows resolved hyperfine couplings with a central metal ion (*e.g.*, Cu^{2+}), the extension of this approach involves an additional sum in eq 6 over the nuclear spin projections of that nucleus.[40] However, we may ignore the unresolved Cu hyperfine interactions of Cu_A in ^1H and ^{14}N ENDOR spectra at 35-GHz frequency because the spread of fields arising from the small hyperfine splittings by the $I = {}^3/_2$ copper nucleus corresponds to a magnetic field range that is small in comparison to the full spread of the entire 35-GHz EPR spectrum.

(39) Rist, G. H.; Hyde, J. S. *J. Chem. Phys.* **1970**, *52*(9), 4633–4643.
(40) Hoffman, B. M.; Gurbiel, R. J. *J. Magn. Reson.* **1989**, *82*, 309–317.

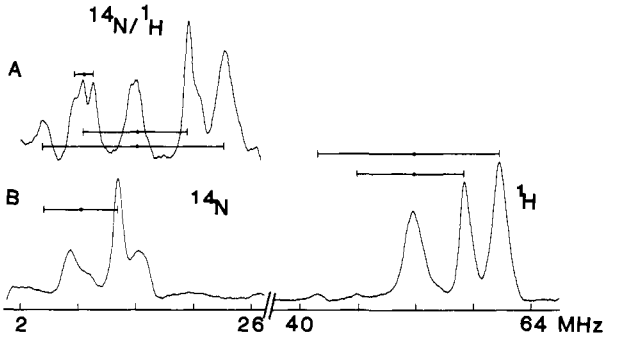

Figure 1. ENDOR spectra of bovine heart cytochrome aa_3 taken near g_2: (A) X-band ENDOR spectrum (9.5 GHz) showing overlapping ^1H and ^{14}N resonances, (B) 35-GHz ^{14}N ENDOR spectrum, and (C) 35-GHz ^1H ENDOR spectrum. Conditions: (A) $H = 0.3333$ T, temperature = 2 K, microwave power = 6 μW, 100-kHz field modulation, modulation amplitude = 0.5 mT, radiofrequency power = 10 W, rf scan rate = 10 MHz/s, 90 scans; (B) conditions are the same as in A except $H = 1.2475$ T, 35.3 GHz, microwave power = 0.5 mW, modulation amplitude = 0.6 mT, rf power = 20 W, rf scan rate = 6 MHz/ s, 260 scans; and (C) conditions are the same as in B except $H = 1.2200$ T, modulation amplitude = 0.25 mT, 90 scans.

We emphasize here that the conceptual utility of this approach, where the integration along s_g selects precisely those orientations that contribute to the ENDOR spectrum and ignores all others, is coupled with the computational advantage that it reduces the simulation procedure to a single, rather than a double, integral.

The above equations in general are adequate for simulating ENDOR spectra and determining hyperfine and quadrupole tensors. However, in some cases, to achieve final simulations of experimental ENDOR spectra, the restriction in eq 6 to a δ-function EPR pattern must be relaxed. The complete expression for the relative ENDOR intensity at frequency ν, for an applied field set to a particular g-value, involves the convolution of ${}^{\delta}I(\nu,g)$, the EPR envelope function derived by Kneubühl (43), $S(g)$, and a component EPR line shape function, $R(g,g')$:

$$I(\nu,g) = \int_{g_{min}}^{g_{max}} dg'\, S(g')\,{}^{\delta}I(\nu,g')R(g,g') \qquad (7)$$

This theory has been implemented as a QUICKBASIC program available from the authors. The ENDOR frequencies employed in this program do not use the simplifications of eqs 1 and 3. Instead, those for protons ($I = {}^1/_2$) use the expressions of Thuomas and Lund;[41] those for ^{14}N ($I = 1$) use exact expressions for the energies as presented by Muha.[42,43] The component line shape functions L and R both were taken as Gaussians and the line widths as isotropic. In applications such as those discussed below, the hyperfine enhancement factor in eq 6 usually could be ignored ($e(\nu) = 1$).

Results

Comparison of X-Band and 35-GHz ENDOR of Cu_A. The X-band ENDOR spectra of Cu_A for all species show overlapping ^1H and ^{14}N resonances. An example is the spectrum of beef cytochrome aa_3 obtained by monitoring the X-band (9.5-GHz) EPR signal at g_2 (Figure 1A). The intense proton pattern is centered at $\nu_H = 14.7$ MHz. Weakly coupled protons give rise to hyperfine splittings in the range of 0–3 MHz; strongly coupled protons, presumably from $-CH_2$ of cysteine, exhibit hyperfine splittings in the range of 11–20 MHz. In addition to the proton resonances, there is a pair of features centered at ~9 MHz that can be assigned to a nitrogenous ligand (N1) because they comprise a Larmor-split doublet centered at $A(N1)/2 \simeq 8.6$ MHz and separated by $2\nu_N = 2.05$ MHz at 9.5 GHz (eq 1). This assignment is consistent with the initial ENDOR studies[12] in which two microwave frequencies in the X-band range were used to assign the ^{14}N and ^1H resonances of beef cytochrome *c* oxidase. Subsequent ENDOR experiments[13] using yeast cytochrome *c*

(41) Thuomas, K.-Å.; Lund, A. *J. Magn. Reson.* **1975**, *18*, 12–21.
(42) Muha, G. M. *J. Chem. Phys.* **1980**, *73*(8), 4139–4140.
(43) Muha, G. M. *J. Magn. Reson.* **1982**, *49*, 431–443.

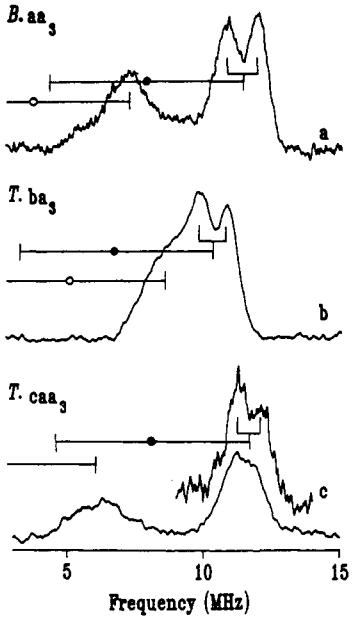

Figure 2. Single-crystal-like (g_1 = 2.18) 35-GHz ^{14}N ENDOR spectra: (a) beef cytochrome aa_3, (b) *Thermus* cytochrome ba_3, and (c) *Thermus* cytochrome caa_3. Conditions: microwave power = 0.5 mW, modulation amplitude = 0.32 mT, radiofrequency power = 10 W, rf scan rate = 2.5 MHz/s. The assignment to $A(N1)/2$ (●) and $A(N2)/2$ (○) and twice the Larmor frequency (|—|) are shown for the two nitrogen ligands.

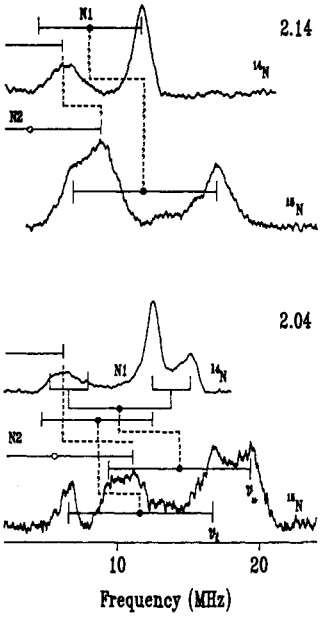

Figure 3. 35-GHz ENDOR spectra of *Thermus* cytochrome caa_3 at g = 214 (upper) and g = 2.04 (lower) from both natural-abundance (^{14}N) enzyme and [^{15}N]histidine enzyme. The assignment to $A(^{14,15}N1)/2$ and $A(^{14,15}N2)/2$ and the magnitudes of $2\nu(^{14}N)$ and $2\nu(^{15}N)$ are indicated as in Figure 2. The dashed lines connect $A(^{14}N)/2$ and $A(^{15}N)/2$ through the ratio of their nuclear g-factors (eq 2). Conditions: **B** = 1.67 and 1.28 T, microwave power = 320 μW, modulation amplitude = 0.25 mT, radiofrequency power = 20 W, scan rate = 2 MHz/s, 4000 scans for [^{15}N]histidine enzyme.

oxidase that incorporated [^{15}N]histidine and [^{2}H]cysteine identified at least one histidine and one cysteine as ligands to Cu_A. However, the presence of the absence of a second histidine or an additional cysteine ligand could not be established at X-band because the ^1H and ^{14}N resonances are so strongly overlapped.

ENDOR experiments on Cu_A performed at 35 GHz eliminate this problem. As shown in the spectrum taken near g_2 for cytochrome aa_3 (Figure 1B), at this microwave frequency the center of the ^1H ENDOR pattern falls at ν_H = 51.9 MHz and the proton pattern shifts unchanged to the radiofrequency range, 40–60 MHz. This provides an unobscured view of the ^{14}N resonances in the 0–40-MHz range, which in this case remain centered at $A(N1)/2$ (eq 1), but with the separation of the ν_+ and ν_- features increased to $2\nu_N$ = 7.5 MHz. The $\nu_+(N1)$ peak seen at ~10 MHz in the X-band spectrum is correlated through eq 1 with the 35-GHz ν_+ peak at ~12 MHz. The $\nu_-(N1)$ partner seen at X-band is much weaker at 35 GHz; in many cases, the ν_- features are not observable. In the absence of overlap with the ^1H signals, additional ^{14}N ENDOR features are seen at 35 GHz that were previously obscured at X-band. For the spectrum of the beef enzyme (see below), these include a shoulder at ~15 MHz on the high-frequency edge of the sharp $\nu_+(N1)$ peak as well as a newly observed resonance at ~8 MHz. It is demonstrated below that this latter feature corresponds to the ν_+ signal for a second nitrogen ligand to Cu_A, $^{14}N2$.

35-GHz $^{14,15}N$ ENDOR of Cu_A. The Cu_A in all three enzymes have qualitatively similar ^{14}N ENDOR patterns. Figure 2 shows ^{14}N ENDOR spectra taken near the low-field g_1 edge of the EPR spectra for each of the three enzymes. In each of these highly resolved spectra, there is a ν_+ feature at ~11 MHz that is assignable to a nitrogenous ligand, N1 with $A_3(N1) \simeq$ 13–16 MHz depending on the enzyme and with a resolved quadrupole splitting of $3P(N1) \simeq 1$ MHz. An additional feature at ~6–8 MHz is assignable to a second ligand, N2 with substantially smaller coupling, $A_3(N2) \simeq$ 7–10 MHz. These assignments have been corroborated through the study of Cu_A in cytochrome caa_3 taken at slightly higher field, where the N1 quadrupole splitting has collapsed (Figure 3), shows a sharp peak at ~12 MHz and a second one at ~6 MHz. The ^{15}N ENDOR spectrum of caa_3 shows a line at ~17 MHz, a second feature with a peak at ~9 MHz, and a well-defined shoulder at ~7 MHz (Figure 3). As indicated, the features at 17 and 7 MHz are partners of a $^{15}N1$ doublet; the 11-MHz peak is the ν_+ feature for $^{15}N2$. The figure illustrates that the ^{15}N and ^{14}N ENDOR spectra are in good agreement when their frequencies are related through use of eq 2. This confirms the above ^{14}N assignment of two nitrogenous ligands and demonstrates that both ligands are histidyl imidazoles. For completeness, we emphasize that $A(N2)$ for Cu_A is far too large to arise from the remote N of the N1 histidyl ligand, and therefore, N2 must be directly coordinated to Cu. We note that the ^{15}N ENDOR spectrum was collected on a sample of ~20-μL volume that contained ~20 μM of Cu_A spins!

It is possible to analyze both hyperfine and quadrupole tensors for N1 if one performs a complete study of the ^{14}N ENDOR field dependence;[37] this has been done for all three enzymes with representative data for cytochrome aa_3 being presented in Figure 4. As the observed g-value is decreased from $g = 2.18 \simeq g_1$, the quadrupole splitting of N1 is first lost and the resulting intense $\nu_+(N1)$ peak shifts to a slightly higher radiofrequency. A shoulder emerges on the high-frequency edge of the spectrum and becomes a resolved peak by $g \simeq 2.04$. As the observed g-value decreases beyond $g \simeq 2.02$ toward g_3, this feature retreats to low frequency. As g approaches g_3, the single-crystal-like ENDOR spectrum for N1 again exhibits a quadrupole-split pair of $\nu_+(N1)$ peaks at $\nu \simeq 13$ MHz.

The splitting of $\nu_+(^{14}N1)$ into two peaks at intermediate fields (g-values) could arise from anisotropy in the hyperfine interaction, from the quadrupole interaction, or from a combination of the two; the ^{14}N ENDOR data are not susceptible to a unique interpretation. However, comparison of ^{14}N and ^{15}N ENDOR spectra at g_2 = 2.04 allows an unambiguous determination. As shown in Figure 3, the $\nu_+(^{15}N)$ feature at $\nu \simeq$ 16–20 MHz exhibits two peaks, $\nu_l(^{15}N) \simeq 16.8$ MHz and $\nu_u(^{15}N) \simeq 19.4$ MHz. Through eq 2, ν_l corresponds to one $\nu_+(^{14}N)$ peak at 12.5 MHz and ν_u corresponds to a quadrupole-split $\nu_+(^{14}N1)$ pair centered at ~14 MHz, with a quadrupole splitting of $3P \simeq 3$ MHz. Thus, the two resolved $\nu_+(^{15}N1)$ features are a manifestation of hyperfine

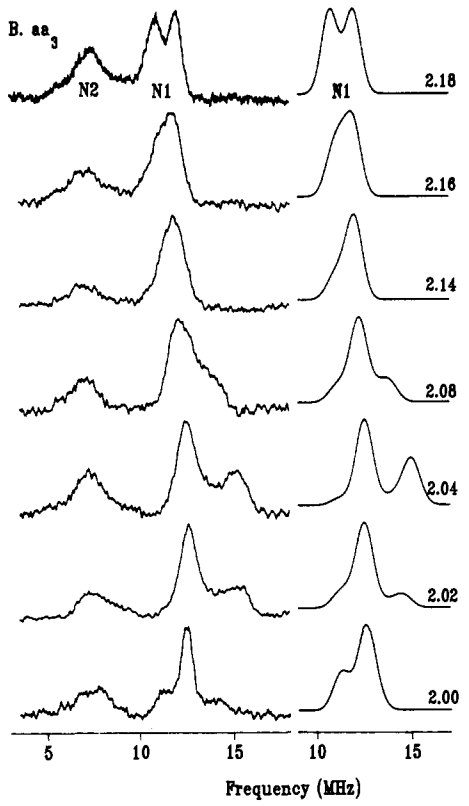

Figure 4. 35.3-GHz ^{14}N ENDOR of beef cytochrome aa_3 at g-values indicated. Conditions: same as those in Figure 2. The corresponding simulations of the ν_+ features for N1 are shown on the right; they employ the hyperfine interaction parameters in Table I.

anisotropy, in that the superposition of resonances from the g = 2.04 subset of orientations exhibits distinct ν_+ features associated with two different orientations within the subset and that these have correspondingly different hyperfine couplings. The ^{14}N–^{15}N ENDOR comparison further shows that one of the $\nu_+(^{14}N)$ features is split by the quadrupole interaction. Consideration of the orientations that give rise to the ENDOR signal at $g = g_2$ = 2.04[44] shows that the ν_u features are associated with molecules where the external field lies along the g_2 axis. The ν_l peak also arises from molecules with $g = g_2$ but from those where the field pierces the unit sphere near the intersection of the meridian joining g_3 = 1.99 and g_1 = 2.18 with the curve s_g (g = 2.04); this intersection lies ~27° out of the g_2–g_3 plane.

Through use of the insights gained from the ^{14}N–^{15}N ENDOR comparisons, the principal values and relative orientations of the ^{14}N ENDOR hyperfine and quadrupole coupling tensors for N1 of the three Cu_A sites have been determined from simulations of a full set of ENDOR spectra using the equations presented above. As illustrated for cytochrome aa_3 (Figure 4), for each enzyme, the experimental spectra can be reproduced well by simulations that employ an approximately axial A(N1) tensor with the unique tensor axis lying roughly along g_2. The P(N1) tensor is taken to be coaxial with A(N1), as seen in single-crystal ENDOR studies of the imidazole bound to Cu(II) in Cu(II)-doped L-histidine·(DCl)·(D_2O)[45] and of Met-myoglobin (Mb);[46] the largest quadrupole coupling (P_{max}) is found to lie along the unique hyperfine axis, as is true for the two reference systems (Table I). Table I contains the N1 tensor components and orientations for all three Cu_A sites. The principal components of the quadrupole tensor match well with those for the Cu(II)-doped histidine crystal[45] as well as for the coordinated histidyl imidazole in Met-myoglobin.[46] Thus, as might be expected, to a *first* approximation these parameters are a property of the metal-bound ligand itself. However, nuclear quadrupole resonance data show that the difference between P_{max} for the ^{14}N of imidazole bound to Cu(II) and to Fe(III) represents significant differences in σ-electron donation by imidazole.[47]

The unique axis of the $^{14}N1$ hyperfine tensor and the largest quadrupole coupling, which are parallel, should lie along the Cu_A–N1 bond direction. From the results presented in Table I, this indicates that the Cu–N1 bond lies roughly along g_2 = 2.04; it is in the g_1–g_2 plane, *ca.* 15° out of the g_2–g_3 ($g_\perp$) plane, namely ~15° out of the plane perpendicular to the unique (g_1) **g**-tensor axis (Figure 5). This suggests a tetrahedral distortion away from a planar ligand geometry. For comparison, the limit of tetrahedral geometry would put N1 out of plane by ~35°. The smallest quadrupole coupling for a transition-ion-bound histidyl ^{14}N lies normal to the imidazole ring (*cf.* refs 45 and 46) as this value lies roughly along g_1; the simulations indicate that the plane of the N1 ring lies approximately in the g_2–g_3 plane.

The average (isotropic) hyperfine coupling for the N1 histidine in the three enzymes is roughly two-fifths of that seen for [Cu(imidazole)$_4$]$^{2+}$,[48] one-half of that for the Cu-doped histidine crystal,[45] and three-fifths of that seen for the more strongly coupled N1 histidine bound to the type 1 Cu(II) of azurin[33] (Table I). The N1 hyperfine tensors for Cu_A of cytochromes aa_3 and caa_3 are essentially identical; the tensor components for cytochrome ba_3 are *ca.* 10–20% less. Ignoring this (significant) difference, then, analysis of the isotropic and anisotropic components of the N1 hyperfine tensors for Cu_A, as discussed elsewhere,[36] indicates a 2s(N1) spin density of *ca.* 1%, a 2p(N1) spin density of *ca.* 2%,[49] and a hybridization at the N1 that approximates to sp^2. The total spin density of *ca.* 3% on N1 of Cu_A is *ca.* one-half of that estimated for the N1 of azurin.

The lower intensity ENDOR resonance for the second ^{14}N, N2, appears at $\nu_+ \simeq 7$ MHz in the g_1 single-crystal spectra for beef cytochrome aa_3 (Figures 1B; 2A, and 4, left), at $\nu_+ \simeq 6.5$ MHz for *Thermus* cytochrome caa_3 (Figure 2C), and at $\nu_+ \simeq$ 9 MHz for *Thermus* cytochrome ba_3 (Figure 2B). As with N1, only the high-frequency half (ν_+) of the N2 pattern is clearly visible, but unlike N1, a quadrupole splitting is never resolved in the g_3 or g_1 single-crystal-like spectra of N2. The field dependencies of the N2 resonance for the three enzymes appear to follow the same general pattern shown by N1, with the difference that the shoulder that swings to higher frequency as g approaches g_2 never becomes an actual peak for N2. The data for N2 of beef cytochrome aa_3 (Figure 4) roughly can be described and an axial A tensor whose principal values are *ca.* one-half of those for N1 and with a quadrupole tensor that is similar to that for N1. However, because of the poor resolution as well as the possible overlap with ν_-(N1) at some fields, there were no serious attempts at simulations. As with N1, there appears to be a correspondence between g_2 and the unique hyperfine tensor component for N2 (Table I). This suggests that the Cu–N2 bond also lies roughly along g_2, which would imply that N1 and N2 are *trans* (Figure 5). However, the poor resolution for N2 requires that this suggestion be made cautiously. The ν_+ features of N2 of *Thermus* cytochromes caa_3 and ba_3 appear at *ca.* 6.5 and 9 MHz, respectively, at all observing g-values (data not shown), and no shoulder can be resolved at any of these g-values. Thus, the ^{14}N coupling to N2 for *Thermus* caa_3 and ba_3 is not distinguishable from isotropic, with A(N2) ≃ 6 and 10.5 MHz, respectively. The N2 histidyl ligands have ^{14}N couplings *ca.* one-half of those of N2 for azurin (Table I).

(44) Doan, P. E.; Hoffman, B. M., unpublished.
(45) McDowell, C. A.; Naito, A.; Sastry, D. L.; Cui, K. S.; Yu, S. X. *J. Mol. Struct.* **1989**, *195*, 361–381.
(46) Scholes, C. P.; Lapidot, A.; Mascarenhas, R.; Inubushi, T.; Isaacson, R. A.; Feher, G. *J. Am. Chem. Soc.* **1982**, *104*(10), 2724–2735.
(47) Ashby, C. I. H.; Cheng, C. P.; Brown, T. L. *J. Am. Chem. Soc.* **1978**, *100*, 6057–6083.
(48) Van Camp, H. L.; Sands, R. H.; Fee, J. A. *J. Chem. Phys.* **1981**, *75*(5), 2098–2107.
(49) Reference parameters are taken from Morton, J. R.; Preston, K. F. *J. Magn. Reson.* **1978**, *30*, 577–582.

Table I. ^{14}N Hyperfine (A) and Quadrupole (P) Tensors (MHz) of Histidylimidazole Ligands N1 and N2 to Cu_A of Beef Cytochrome aa_3 and *Thermus* Cytochromes caa_3 and ba_3 and of Reference Compounds

		beef aa_3		*Thermus* caa_3		*Thermus* ba_3		azurin[a]	Cu^{II}–histidine[b,c]		Mb[d,c]
		A	P[e]	A	P[e]	A	P[e]	A	A	P	P
N1[f]	x	16	0.5	16	0.7	14.4	0.6		28.9	0.75	0.81
	y	15.6	0.4	15	0.3	13.8	0.3	27	28.9	0.17	0.31
	z	20.3	–0.9	20.2	–1.0	18	–0.9		37.7	–0.92	–1.12
	ω[g]	~15°		~15°		~15°					
N2[h]	x	8									
	y	7	*i*	6[j]		10.5[j]		17			
	z	11	~1								

[a] Werst *et al.*, 1991.[33] [b] Histidylimidazole bound to Cu(II) in Cu(II)-doped histidine(DCl)·(HDO). The other ligands to Cu(II) are two Cl^- and an amino nitrogen.[45] As presented here, A_1 and A_2 are the average of the almost indistinguishable experimental values. Axes have been relabeled according to our conventions. [c] Single-crystal ENDOR data show the (A_z,P_z) point along the N1–metal bond and that P_y is normal to the imidazole ring. [d] Histidylimidazole bound to the heme iron of ferrimyoglobin.[46] Note that ref 46 uses the symbol Q, rather than P, in its spin-Hamiltonian, which conventionally is written $I\cdot P\cdot I$. In conventional notation, Q differs from P by a factor of 2; $P = 2Q$. [e] Our measurements determine relative signs of P_i but do not distinguish between ±P; the choice of signs is made by comparison with the two reference systems. [f] N1: hyperfine uncertainties, ±0.5 MHz; quadrupole, ±0.1 MHz. [g] Orientation of N1: A_x, and P_x lie along g_3; A_z and P_z are rotated around g_3 away from the g_2 axis by the angle ω. [h] For beef aa_3, the A and P tensors appear to be roughly coaxial with the g-tensor. Uncertainties: hyperfine, ~±1 MHz; quadrupole, ±0.15 MHz. [i] Unresolved. [j] The couplings are either isotropic or nearly so for caa_3 and ba_3.

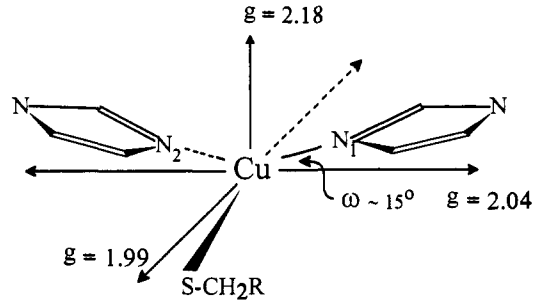

Figure 5. Sketch of orientations of histidylimidazoles relative to the g-tensor of Cu_A drawn as a mononuclear site (but see Discussion section) and including the one cysteine known to be a ligand. The dashed line to N2 signifies a lower confidence as to its placement (see text).

35-GHz ^1H ENDOR of Cu_A. The ^1H ENDOR of Cu_A in all three enzymes shows at least two, and possibly more, strongly coupled proton signals.[11,12,50] These have been observed previously, the isotope-labeling work of Stevens *et al.*[13] favors the interpretation that they arise from β-methylene protons of cysteinyl ligand(s). Because our present ^1H ENDOR spectra do not make definitive additions to previous arguments and because we are currently preparing samples of the bacterial cytochromes labeled with [^2H]cysteine and [^{13}C]cysteine, we will forego discussion of these signals at this time.

X-Band $^{63,65}Cu$ ENDOR. ENDOR signals from $^{63,65}Cu$ of Cu_A have been detected for the three enzymes. Each of the X-band spectra obtained by monitoring the g_2 EPR signal (Figure 6) shows intense resonances in the 15–25-MHz region due to the ν_+ features of strongly coupled protons and a broad, poorly resolved feature in the range of 30–70 MHz that we assign to $^{63,65}Cu$. For both *Thermus* cytochrome caa_3 and beef cytochrome aa_3, the copper ENDOR signal (Figures 6B and 6C, respectively) is of opposite phase to the ^1H signals. This phase reversal has been reported earlier for Cu_A[11] and also was observed for the blue copper proteins.[51] This undoubtedly represents a superposition of signals from the two Cu isotopes ^{63}Cu (69%) and ^{65}Cu (31%), but they differ minimally with regard to nuclear g-factor and quadrupole moment (~6.5%), and so we discuss only the average, observed, spin-Hamiltonian parameters. For both proteins, the center frequency of the pattern gives $A(Cu) \simeq 104$ MHz. The six-line pattern predicted by eq 1 for the quadrupole interaction is not resolved, but the breadth of the signal at g_2 in Figures 6B and 6C corresponds to $3P(Cu) \simeq 3$ MHz. In contrast, the copper

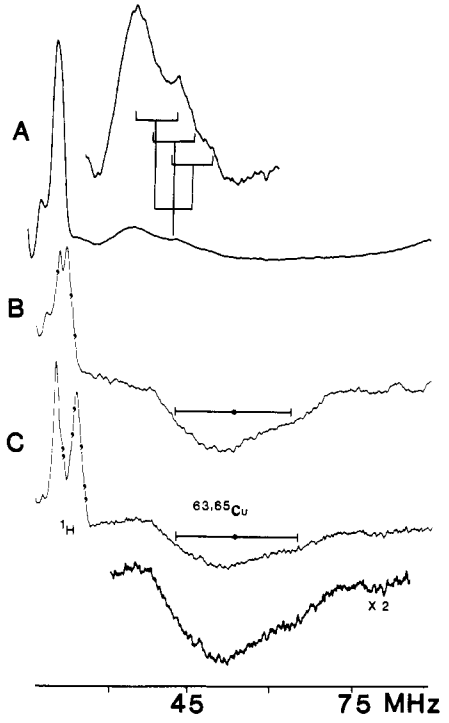

Figure 6. Copper X-band (9.5-GHz) ENDOR spectra: (A) *Thermus* cytochrome ba_3, (B) *Thermus* cytochrome caa_3, and (C) beef cytochrome aa_3. Conditions: T = 2 K, microwave power = 6 μW, 100-kHz field modulation, modulation amplitude = 0.5 mT, radiofrequency power = 10 W, rf scan rate = 15 MHz/s, (A) H = 0.3355 T, (B) H = 0.333 T, (C) H = 0.333 T.

ENDOR signal of *Thermus* cytochrome ba_3, shown in Figure 6A, has the same phase as that of the ^1H signals, and its center frequency corresponds to a hyperfine coupling of $A(Cu) \simeq 78$ MHz, significantly smaller than those for the other two enzymes. The resolution of the Cu ENDOR signal in Figure 6A allows us to propose the assignment shown, where the three-line pattern due to quadrupolar splitting by the $I = {}^3/_2$ Cu nucleus ($3P(Cu) \simeq 4$ MHz) is in turn split into doublets by the nuclear Zeeman interaction. The $^{63,65}Cu$ couplings observed by ENDOR for the Cu_A site are all noticeably smaller than those for the type 1 Cu centers, $A(Cu) \simeq 150$–200 MHz,[51] consistent with the lack of resolved Cu couplings in the EPR spectra are associated with a binuclear Cu center would require that the Cu(I)/Cu(II) ions have very nearly equal couplings, which would require symmetrical valence delocalization.

(50) Gurbiel, R. J.; Werst, M. M.; Surerus, K. K.; Fee, J. A.; Hoffman, B. M., unpublished.
(51) Roberts, J. E.; Brown, T. G.; Hoffman, B. M.; Peisach, J. *J. Am. Chem. Soc.* **1980**, *102*(2), 825–829.

```
Bos taurus            PMEMTIRMLVSSEDVLHSWAVPSLGLKTDAIPGRLNQTTLMSSRPGLYYGQCSEICGSNHSFMPI
S. cerevisiae         PVDTHIRFVVTAADVIHDFAIPSLGIKVDATPGRLNQVSALIQREGVFYGACSELCGTGHANMPI
P. denitrificans      PVGKKVLVQVTATDVIHAWTIPAFAVKQDAVPGRIAQLWFSVDQEGVYFQGCSELCGINHAYMPI
T. thermophilus caa3  PAGVPVELEITSKDVIHSFWVPGLAGKRDAIPGQTTRISFEPKEPGLYYGFCAELCGASHARMLF
T. thermophilus ba3   PQGAEIVFKITSPDVIHGFHVEGTNINVEVLPGEVSTVRYTFKRPGEYRIICNQYCGLGHQNMFG
                                      *                                  *   *   *  *
                      126                                                           191
```

Figure 7. Cu_A motif found in subunit II and subunit IIc sequences of cytochrome *c* oxidases. The asterisk indicates conserved residues that are potential metal ligands in the Cu_A site. The numbering is from the bovine protein. Sequences except that from cytochrome ba_3 are found in Mather *et al.*, 1991.[22] The partial sequence of cytochrome ba_3 subunit II is from the Ph.D. Thesis of Keightley (1993).[25]

Discussion

Previous work has shown that the Cu_A sites in cytochromes aa_3, caa_3, and ba_3 have similar electronic, EPR, and EXAFS spectra,[17,24,31,52] and the present work shows that this extends to the higher resolution provided by 35-GHz ENDOR spectroscopy. In the oxidized form of the enzyme, each of the three Cu_A sites exhibits two nitrogen ligands with quite different hyperfine coupling tensors. Examination of cytochrome caa_3 that incorporates $[\delta,\epsilon\text{-}^{15}N_2]$histidine proves that in this case, and presumably all cases, the two nitrogens arise from histidyl ligands to Cu. Our theory for simulating polycrystalline ENDOR spectra has allowed us to determine both hyperfine and quadrupole tensors for N1 and to approximate them for N2 of the three enzymes. The resolution of quadrupole couplings for the imidazole ^{14}N directly bonded to Cu(II) is rare for biological Cu centers. The principal components of the **A** and **P** tensors for N1 and N2 do not differ significantly among the three enzymes, except that the **A**(N1) components for ba_3 are *ca.* 10% less than those for the other two. The N1 quadrupole tensors are quite comparable to those found earlier for the imidazole nitrogen bound to Cu(II) (Table I). Taken together, these observations indicate a common ligand composition and geometric arrangement of Cu_A in the three enzymes.

The idea of $(His)_2$–$(Cys)_2$ coordination in the Cu_A site continues to be a widely accepted working hypothesis.[53] Central to this idea is the assumption that Cu_A is associated with subunit IIc through coordination to a region of sequence we call the Cu_A motif. Figure 7 shows the sequences of this region taken over a wide phylogenetic range and including the three enzymes used in this study.[54] Note there are two conserved histidine residues, two conserved cysteine residues, and one conserved methionine residue that could serve as ligands to Cu_A. Recent sequence analysis and site-directed mutation studies of subunits I have pretty much confirmed the notion that the Cu_A site resides in subunit II by showing that the six (possibly seven) conserved histidine residues in the latter subunit coordinate cytochrome *a*(*b*), cytochrome $a_3(o)$, and Cu_B.[55] The 35-GHz ENDOR data on caa_3 prepared with ^{15}N-labeled histidine show unequivocally that two histidines are coordinated to Cu_A. These ligands must be provided by subunit IIc, and the only conserved histidine residues in subunit IIc are in the Cu_A motif. Therefore, these two histidines must be those in the Cu_A motif.

For each of the enzymes studied here, the $[^{14}N]$histidine and $^{63,65}Cu$ hyperfine splittings are small relative to the values for type 1 copper sites, which have three strongly coordinated ligands, $(His)_2(Cys)$. The hyperfine couplings for the histidine nitrogens coordinated to type I copper centers are in the 17–47-MHz range[33] and thus can even exceed $A = 42$ MHz for $[Cu(imidazole)_4]^{2+}$,[48] whereas for the terminal oxidases examined here, the ^{14}N hyperfine couplings are in the range of 6–23 MHz. As a specific example (Table I) the average hyperfine couplings for N1 and N2 of Cu_A are, respectively, *ca.* three-fifths and one-half of those for N1 and N2 of azurin. Similarly, the ^1H couplings for the methylene protons of Cu_A in these oxidases are in the range of 5–19 MHz (Figure 1)[11,12,50] in comparison to the 16–31-MHz range for the type I centers.[33] Finally, $^{63,65}Cu$ hyperfine couplings for Cu_A are ~100 MHz (~80 MHz for ba_3), versus 150–200 MHz for blue copper. The Cu hyperfine data are consistent with the idea of greater spin delocalization from Cu to the ligand in the Cu_A site compared to in blue copper sites, as originally suggested by Peisach and Blumberg.[7] However, the hyperfine couplings to ligand nuclei in Cu_A are smaller than those in type 1 (blue) Cu, which means that there is less spin *per* ligand in Cu_A than in blue copper. Thus, it is likely that the key difference between the two classes of Cu centers is that Cu_A has one more strongly coordinating ligand with high spin density, quite possibly a mercaptide sulfur, in addition to the $(His)_2(Cys)$ coordination of blue copper. (*cf.* ref 53, the MO model.)

The ENDOR data also provide initial three-dimensional structural information about the coordination environment. The more strongly coupled nitrogen ligand N1 is well-characterized for each of the three enzymes, the analysis indicating that the Cu–N1 bond lies roughly along g_2 and ~15° out of the $g_\perp$ (g_2–g_3) plane. The orientation of the second, less strongly coupled nitrogen ligand N2 is not well-determined, but for cytochrome aa_3 there is a suggestion that it may be roughly *trans* to N1.

The data further can be used to discuss the alternate proposal that Cu_A is in reality a binuclear Cu center. This view requires a mixed-valence, formally Cu^{II}/Cu^{I}, cluster that exhibits valence delocalization so that the two ions exhibit very nearly identical Cu hyperfine coupling.[8] However, there are only two histidines available to coordinate to metal ions at this site, and the 35-GHz ENDOR shows that their bonds to Cu, as reflected in the ^{14}N hyperfine coupling tensors, are very different. Thus, if the Cu_A site is indeed binuclear, the $(Cu_2)^{3+}$ unit nonetheless exhibits quite unsymmetrical coordination.

Acknowledgment. We thank C. I. Nitsche and P. Springer for assistance in protein purification and sample preparation and Dr. J. Andrew Keightley for permission to present the deduced amino acid sequence of cytochrome ba_3 subunit II in advance of publication. This work was supported by the U.S. Public Health Service grants HL13531 to B.M.H., GM35342 to J.A.F., and GM22432 to S.I.C., the Stable Isotope Resource at Los Alamos (RR02321), and the National Science Foundation grant DMB-8907559 to B.M.H. Work carried out at Los Alamos was done under the auspices of the U.S. Department of Energy. S.M.M. is the recipient of a National Research Service Predoctoral Award.

(52) Chan, S. I.; Bocian, D. F.; Brudvig, G. W.; Morse, R. H.; Stevens, T. H. In *Cytochrome Oxidase*; King, T. E., Ed.; Elsevier/North Holland Biomedical Press: Amsterdam, 1979; pp 177–188.
(53) Chan, S. I.; Li, P. M. *Biochemistry* **1990**, *29*(1), 1–12.
(54) It is now known with certainty that cytochrome ba_3 is at least a two-subunit enzyme, being a homolog of the heme–copper oxidase family (see refs 25 and 26, above).
(55) For review, *cf.*: Fee, J. A.; Yoshida, T.; Surerus, K. K.; Mather, M. W. *J. Bioenerg. Biomemb.* **1993**, in press.